

1 **Reconstructing the annual mass balance of glacier Echaurren Norte (Central Andes,**  
2 **33.5°S) using local and regional hydro-climatic data**

4 **M.H. Masiokas<sup>1</sup>\*, D.A. Christie<sup>2,3</sup>, C. Le Quesne<sup>2</sup>, P. Pitte<sup>1</sup>, L. Ruiz<sup>1</sup>, R. Villalba<sup>1</sup>, B.H.**  
5 **Luckman<sup>4</sup>, E. Berthier<sup>5</sup>, S.U. Nussbaumer<sup>6</sup>, A. González-Reyes<sup>7</sup>, J. McPhee<sup>8</sup>, G. Barcaza<sup>9</sup>**

7 <sup>1</sup> Instituto Argentino de Nivología, Glaciología y Ciencias Ambientales (IANIGLA),  
8 CCT- CONICET Mendoza, C.C. 330, (5500) Mendoza, Argentina

9 <sup>2</sup> Laboratorio de Dendrocronología y Cambio Global, Instituto de Conservación Biodiversidad y  
10 Territorio, Facultad de Ciencias Forestales y Recursos Naturales, Universidad Austral de Chile,  
11 Valdivia, Chile.

12 <sup>3</sup> Center for Climate and Resilience Research (CR)<sup>2</sup>, Chile.

13 <sup>4</sup> Department of Geography, University of Western Ontario, Canada.

14 <sup>5</sup> LEGOS, CNRS, Université de Toulouse, France

15 <sup>6</sup> Department of Geography, University of Zurich, and Department of Geosciences, University of  
16 Fribourg, Switzerland.

17 <sup>7</sup> Departamento de Geología, Facultad de Ciencias Físicas y Matemáticas, Universidad de Chile.

18 <sup>8</sup> Departamento de Ingeniería Civil, Facultad de Ciencias Físicas y Matemáticas, Universidad de  
19 Chile.

20 <sup>9</sup> Dirección General de Aguas (DGA), Santiago, Chile.

21

22 \* Correspondence to: [mmasiokas@mendoza-conicet.gob.ar](mailto:mmasiokas@mendoza-conicet.gob.ar)

23 Tel.: +54-261-5244264

24 Fax: +54-261-5244201

25

26

27 **Abstract**

28 Despite the great number and variety of glaciers in southern South America, *in situ* glacier mass  
29 balance records are extremely scarce and glacier-climate relationships are still poorly understood  
30 in this region. Here we use the longest (>35 yrs) and most complete *in situ* mass balance record,  
31 available for glaciär Echaurren Norte in the Andes at ~33.5°S, to develop a minimal glacier  
32 surface mass balance model that relies on nearby monthly precipitation and air temperature data  
33 as forcing. This basic model is able to explain 78% of the variance in the annual glacier mass  
34 balance record over the 1978-2013 calibration period. An attribution assessment identified  
35 precipitation variability as the dominant forcing modulating annual mass balances at ECH, with  
36 temperature variations likely playing a secondary role. A regionally-averaged series of mean  
37 annual streamflow records from both sides of the Andes between ~30° and 37°S is then used to  
38 estimate, through simple linear regression, this glacier's annual mass balance variations since  
39 1909. The reconstruction model captures 68% of the observed glacier mass balance variability  
40 and shows three periods of sustained positive mass balances embedded in an overall negative  
41 trend over the past 105 years. The three periods of sustained positive mass balances (centered in  
42 the 1920s-30s, in the 1980s and in the first decade of the 21<sup>st</sup> century) coincide with several  
43 documented glacier advances in this region. Similar trends observed in other shorter glacier mass  
44 balance series suggest that the glaciär Echaurren Norte reconstruction is representative of larger-  
45 scale conditions and could be useful for more detailed glaciological, hydrological and  
46 climatological assessments in this portion of the Andes.

47

48

49 **1. Introduction**

50 The extra-tropical Andes between  $\sim 23^{\circ}$  and  $55^{\circ}$ S contain a large number and variety of glaciers  
51 ranging from small glacierets at elevations of over 6000 m in the high, arid Andes of northern  
52 Chile and Argentina, to large outlet glaciers that reach the sea in the humid southwestern portion  
53 of Patagonia and Tierra del Fuego. Altogether, these ice masses concentrate the largest  
54 glacierized area in the Southern Hemisphere outside Antarctica and are highly valued as sources  
55 of freshwater, as indicators of climatic change, as tourist attractions, and as environmental and  
56 cultural icons in different sectors of the Andes. As reported for other mountainous areas of the  
57 globe, glaciers in southern South America display a widespread retreating pattern that has been  
58 usually attributed to warmer, and sometimes drier, climatic conditions in this region (Villalba et  
59 al. 2003; Rignot et al. 2003; Rivera et al. 2000, 2005; Masiokas et al. 2008, 2009; Le Quesne et  
60 al. 2009; Pellicciotti et al. 2014). Quantitative assessments of regional glacier mass balance  
61 changes and glacier-climate relationships are, however, seriously hampered by the scarcity and  
62 short length of *in situ* glacier mass balance data and proximal climate records within the Andes.  
63 The latest publication of the World Glacier Monitoring Service (WGMS 2013) reports annual  
64 mass balance measurements for seven extratropical Andean glaciers (five in Argentina, two in  
65 Chile). Four of these records start in 2010 and are for small glaciers and glacierets located ca.  
66 29.30°S, two records are located between 32°-34°S and start in the mid-late 1970s, and the  
67 remaining record from Tierra del Fuego (54.8°S) starts in 2001. Discontinued, short-term glacier  
68 mass balance measurements (see e.g. Popovnin et al. 1999) and recent programs initiated at new  
69 sites (e.g. Rivera et al. 2005; Rabatel et al. 2011; Ruiz et al. 2013) complete the network of direct  
70 glacier mass balance data currently available in southern South America. Although not optimal in  
71 terms of spatial coverage, arguably the single most important limitation of this network is the  
72 short period of time covered by consistent, reliable records. Of the two longest mass balance  
73 series mentioned above (glaciar Echaurren Norte and glaciar Piloto Este in the Central Andes, see  
74 Table 1.1 in WGMS 2013), only the series from Echaurren Norte in Chile (Fig. 1A-C) provides a  
75 complete record spanning more than 35 years. In fact, this series constitutes the longest direct  
76 glacier mass balance record in the Southern Hemisphere (see Escobar et al. 1995a,b; DGA 2010  
77 and WGMS 2013) and is thus a “reference” glacier in the WGMS global assessments. The mass  
78 balance record from glaciar Piloto Este (located ca. 100 km to the north in Argentina; Fig. 1A)

79 covers the 1979-2002 period and contains several data gaps that have been interpolated using  
80 various techniques (Leiva et al. 2007).

81  
82 Many studies dealing with recent climate and glacier changes in southern South America have  
83 pointed out the shortness, poor quality, or absence of climatic records at high elevation sites or in  
84 the proximity of glaciers in the Andes (Villalba et al. 2003; Rivera et al. 2005; Masiokas et al.  
85 2008; Rasmussen et al. 2007; Falvey and Garreaud 2009; Pellicciotti et al. 2014; Vuille et al.  
86 2015). Given the lack of suitable data, many climatic assessments have used records from distant,  
87 low elevation weather stations and/or gridded datasets to estimate conditions and recent climate  
88 variability within the Andean range. It is interesting to note, however, that the amount of hydro-  
89 climatic information (in particular from solid and liquid precipitation, and hydrologic variables)  
90 is comparatively better for those portions of the southern Andes that support large populated  
91 centers and where the water provided by the mountains is vital for human consumption,  
92 agriculture, industries and/or hydropower generation. In these areas, mainly between ca. 29° and  
93 42°S, local and national water resource agencies have monitored a well-maintained network of  
94 hydrologic and meteorological stations for several decades (see e.g. Masiokas et al. 2006, 2010).  
95 The data from the stations in this region are slowly becoming publicly available and are  
96 substantially better in terms of quantity and quality than those for the less populated, more  
97 inaccessible areas in southern Patagonia or in the Desert Andes of northern Chile and Argentina.  
98

99 The Central Andes of Chile and Argentina between ~31° and 35°S (see Lliboutry 1998) have a  
100 mean elevation of about 3500 m with several peaks reaching over 6000 m (Fig. 1A). The climate  
101 of this region is characterized by a Mediterranean regime with a marked precipitation peak during  
102 the cold months (April to October) and little precipitation during the warm summer season  
103 (November to March; Fig. 1D). Almost all of the moisture comes from westerly Pacific frontal  
104 systems, precipitating as rainfall in the Chilean lowlands and as snow in the Andes to the east  
105 (Miller 1976; Aceituno 1988; Garreaud 2009). The snow accumulated in the mountains during  
106 winter remains frozen until the onset of the melt season (usually October-November), producing  
107 a unimodal snowmelt-dominated regime for all rivers originating on either side of the Andes at  
108 these latitudes (Masiokas et al. 2006; Cara et al. in press). This relatively simple configuration  
109 entails some potential benefits for the study and understanding of the hydro-climatic and

110 glaciological processes in this region: First, the strong co-variability between total rainfall  
111 amounts measured in central Chile and winter snow accumulation and river discharges recorded  
112 in the Andes (see Fig. 2) allows the use of a relatively limited number of station records to  
113 capture the main regional hydro-climatic patterns. The strong common signal among these  
114 variables also offers the possibility of inferring or reconstructing selected instrumental data (e.g.  
115 winter snow accumulation, which begins in 1951) using data from other well-correlated variables  
116 with a longer temporal coverage (e.g. Andean streamflow records which are available since  
117 1909). Masiokas et al. (2012) used these relationships to extend Andean snowpack variations  
118 using central Chile rainfall records and precipitation-sensitive tree-ring width series.

119  
120 In contrast to the well-known similarities between precipitation (solid and liquid) and surface  
121 runoff, the spatial and temporal patterns of high-elevation temperature records in the Central  
122 Andes of Chile and Argentina are still poorly understood. Falvey and Garreaud (2009) presented  
123 a detailed assessment of temperature trends over the 1979-2006 period along the western margin  
124 of subtropical South America, reporting a notable contrast between surface cooling (-  
125 0.2°C/decade) in coastal stations and a warming trend of ca. +0.25°C/decade in the Andes only  
126 100-200 km inland. However, only two land stations were available with long enough records  
127 above 2000 m (i.e. El Yeso and Lagunitas stations in Chile at 2475 and 2765 m, respectively), but  
128 radiosonde data from the coastal station Quintero (ca. 33°S) showed comparable positive trends  
129 for the free-troposphere (Falvey and Garreaud 2009). This lack of high elevation surface  
130 temperature data also restricted the recent assessments of Vuille et al. (2015), who focused their  
131 elevation-dependent temperature trend analyses on the region north of 18°S because data were  
132 too sparse farther south.

133  
134 The station El Yeso (33°40'36"S, 70°05'19"W) is located only 10 km south of glacier Echaurren  
135 Norte (Fig. 1B). Mean daily and monthly temperature and total precipitation measurements from  
136 this station are available since 1962 but contain several months with missing data prior to 1977  
137 (temperature) and 1975 (precipitation). Since 1977, both series are practically complete and  
138 updated on a regular basis. To our knowledge, in the entire extra-tropical Andes there is no other  
139 operational meteorological station with such a long and complete record of temperature and  
140 precipitation variations less than a few kilometres from a glacier, which moreover contains the

141 longest ongoing mass balance monitoring program in the Southern Hemisphere. This rare  
142 combination of relatively long, complete climate records near a well-studied glacier site clearly  
143 highlights the importance of this unique location for varied glaciological and climatological  
144 investigations in the southern Andes.

145  
146 In this contribution we use seasonal mass balance records from glacier Echaurren Norte plus  
147 local and regionally-averaged monthly hydro-climatic data to model and reconstruct annual  
148 glacier mass balance changes over the past 105 years. Since only the glacier-wide seasonal and  
149 annual mass balance components are available for ECH, one of the main objectives of the study  
150 was to explore the suitability of simple mass balance models that require a minimum amount of  
151 input data (Marzeion et al. 2012; see also Kaser et al. 2010). Although this simplistic approach  
152 provides limited insight into the intricate physical processes involved in this glacier's intra-  
153 annual mass balance variations, it may, nonetheless, offer a useful starting point to address some  
154 basic (yet still poorly known) questions regarding the glacier's sensitivity to climate variations.  
155 We did not consider a data-intensive approach to measure and model the complex daily energy  
156 and mass balance variations of this glacier (e.g. Pellicciotti et al. 2014) because of the lack of the  
157 high resolution, *in situ* meteorological and glaciological measurements usually required in these  
158 type of analyses. Another primary objective was to use the available, well correlated hydrological  
159 records from this region (Fig. 2) to extend the ECH annual mass balance record and evaluate the  
160 fluctuations of mass balance over a much longer period than that covered by regular glaciological  
161 measurements. Comparisons with other shorter mass balance series and with a record of glacier  
162 advances in this region suggest the resulting time series contain a discernible regional footprint.  
163 Overall, we believe the findings discussed below constitute a substantial improvement in the  
164 understanding of the main patterns and forcings of the glacier mass balance changes in this region  
165 and provide a useful background for more detailed glacio-climatic assessments and modeling  
166 exercises in this portion of the Andes.

167  
168 **2 – Data and Methods**  
169 **2.1. Glacier mass balance data**  
170 Glaciar Echaurren Norte (33°33'S, 70°08'W; hereafter ECH) is located within a southwestern  
171 oriented cirque ~50 km southeast of Santiago de Chile, in the headwaters of the Maipo river basin

172 (Fig. 1A-C). ECH provides water to Laguna Negra, a natural lake that together with the nearby El  
173 Yeso artificial lake constitute crucial water reservoirs for extensive irrigated lands and for the  
174 metropolitan Santiago area in Central Chile.

175

176 Mass balance measurements started at this easily accessible glacier in the austral spring of 1975  
177 under the auspices of Dirección General de Aguas (DGA), the institution in charge of monitoring  
178 and managing water resources in Chile. Summer and winter mass balance data at ECH have been  
179 regularly measured until the present by DGA officials, and have been reported in sporadic  
180 internal documents and scientific publications (Peña and Narbona 1978; Peña et al. 1995;  
181 Escobar et al. 1995, 1997; DGA 2010). These records have also been reported to the WGMS,  
182 from where we obtained the 1975-2012 data used in this manuscript (annual mass balance data  
183 extend to 2013; see WGMS 2013 and [www.wgms.ch](http://www.wgms.ch)). The glacier has thinned in the last decades  
184 and presently consists of small remnants of both clean and debris-covered ice (Fig. 1C). Despite  
185 this evident ice mass loss, the elevation range of the glacier has not changed much since  
186 measurements started in the mid 1970s. According to Peña and Narbona (1978) and Escobar et al.  
187 (1995), in the first years of the mass balance program the glacier covered an area of 0.4 km<sup>2</sup>  
188 distributed over a short elevation range between ca. 3650 and 3880 m asl (Fig. 1C). Over the time  
189 period covered by the mass balance records, no adjustment has been made to incorporate the  
190 changes in surface area of the glacier, and thus the reported values are considered here as  
191 reference-surface mass balance estimates (i.e. the mass balance that would have been observed if  
192 the glacier topography had not changed over the study period; see Cogley et al. 2011).

193

194 Mass balance data from glaciär Piloto Este (hereafter PIL) from 1979-2002 and shorter time  
195 series from small glaciers and glacierets further north in this region are also available from the  
196 WGMS database (Leiva et al. 2007; Rabaté et al. 2011; WGMS 2013; see Fig. 1A and Table 1).  
197 Here we compare the cumulative annual mass balance records of these glaciers as independent  
198 validation measures of the main patterns and temporal trends observed in the measured and  
199 modeled mass balance series from ECH.

200

## 201 **2.2 Minimal glacier mass balance model**

202 A minimal model only requiring monthly temperature and precipitation data (Marzeion et al.  
203 2012) was used to estimate the interannual surface mass balance variations of ECH and to  
204 explore the relative importance of temperature and precipitation variability on the ECH records.  
205 In their publication, Marzeion et al. (2012) used gridded precipitation and temperature data to  
206 calibrate individual models for 15 glaciers with existing mass balance measurements in the  
207 greater Alpine region. The climate data used here come from El Yeso, a permanent automatic  
208 weather station maintained by DGA and located ca. 10 km to the south and 1200 m lower than  
209 ECH's snout (Fig. 1B). The data are freely available at the DGA website ([www.dga.cl](http://www.dga.cl)) and  
210 contain practically complete monthly temperature and precipitation records since 1977 (only four  
211 missing months were filled using their long-term means). The mass balance model can be defined  
212 as follows:

213

$$214 MB = \sum_{i=1}^{12} (\alpha P_i - \mu(\max(0, T_i - T_{melt}))) \quad (1)$$

215  
216 where  $MB$  represents the modeled annual specific mass balance of the glacier,  $P_i$  are monthly  
217 total precipitation values at the El Yeso station, and  $\alpha$  is a scaling parameter introduced to  
218 compensate for the precipitation gradient between the elevation of this station (rounded here to  
219 2500 m) and the front of ECH (fixed at 3700 m in this analysis). We do not differentiate solid vs.  
220 liquid precipitation because at this glacier (and in other high elevation areas in this portion of the  
221 Andes) the bulk of precipitation occurs during the winter months and the fraction of liquid  
222 precipitation is usually minimal compared to the large proportion that falls as snow (see Fig. 1D).  
223 The use of total precipitation values also avoids the additional complexity and uncertainties  
224 involved in differentiating solid from liquid precipitation at this glacier, which is distributed over  
225 a very small altitudinal range (see also Fig. 1C).  $T_i$  represents mean monthly temperatures at El  
226 Yeso extrapolated to the elevation of the glacier front using a constant lapse rate of  $-0.065^{\circ}\text{C}/100$   
227 m, and  $T_{melt}$  is the monthly mean temperature above which melt occurs. As indicated in Marzeion  
228 et al. (2012), the maximum operator ensures that melting occurs only during months with mean  
229 temperatures above  $T_{melt}$ . The parameter  $\mu$  is expressed in  $\text{mm K}^{-1}$  and was introduced to translate  
230 the monthly temperature records into monthly ablation values at the glacier. In order to estimate  
231 the parameters  $\alpha$  and  $\mu$  and validate the final model, we performed a “leave-one-out” cross

232 validation procedure (Michaelsen 1987). In this approach, ECH data for each year between 1977  
233 and 2012 (common period between the El Yeso data and the ECH mass balance series) were  
234 successively excluded and the minimal mass balance model (Eq. 1) calibrated with the remaining  
235 values. At each step the parameters  $\alpha$  and  $\mu$  were first optimized to minimize the root mean  
236 squared error (rmse; Weisberg 1985) of the modeled values, and then used to estimate the mass  
237 balance data omitted that year. This resulted in 36 predicted values which were compared to the  
238 actual annual mass balance observations to compute validation statistics of model accuracy and  
239 error. The exercise showed that the model parameters are relatively time stable:  $\alpha$  ranged between  
240 3.9 and 4.1 (mean value used here = 3.9), whereas  $\mu$  varied between 89.0 and 91.0 mm K<sup>-1</sup> (mean  
241 value used = 90.1 mm K<sup>-1</sup>). The mean estimated value of  $\alpha$  indicates that accumulation at the  
242 glacier is normally about four times larger than the annual precipitation recorded at El Yeso. The  
243 mean estimated value for  $\mu$  is also reasonable and within the range of values reported by  
244 Marzeion et al. (2012) for the 15 glaciers with direct measurements in the European Alps (76-156  
245 mm K<sup>-1</sup>, see their Table 1). Finally, for the sake of simplicity, we prescribed  $T_{melt} = 0^\circ\text{C}$  as  
246 suggested in Marzeion et al. (2012).

247

### 248 **2.3 Glacier mass balance reconstruction**

249 In addition to modeling the interannual mass balance variations of ECH using the temperature  
250 and precipitation data from El Yeso, we also used regionally representative hydroclimatic  
251 indicators to extend the observed glacier mass balance record prior to 1975. The use of these  
252 indicators (regionally-averaged series of winter snow accumulation and mean annual river  
253 discharges; see Masiokas et al. 2006) was supported by visual comparisons and correlation  
254 analyses which showed strong, statistically significant positive associations not only with the  
255 winter record at ECH, but also with the annual mass balance series of this glacier (Table 2 and  
256 Fig. 2). The correlation was also positive but weaker between the summer component at ECH and  
257 the regional snowpack and streamflow series.

258

259 The regionally-averaged record of winter snow accumulation is based on eight selected stations  
260 located in the Chilean and Argentinean Andes between 30° and 37°S (Fig. 1A and Table 3). The  
261 dataset has been updated from the one used by Masiokas et al. (2012) and contains the longest  
262 and most complete snowpack records in this region. Prior to computing the regional average, the

263 individual series were expressed as percentages from their 1981-2010 climatology mean values.  
264 A similar approach was used to develop a regional record of mean annual (July-June) streamflow  
265 variations. This series was calculated using monthly data from 11 gauging stations with the  
266 longest and most complete records in this portion of the Andes (Fig. 1A and Table 3). The  
267 resulting snowpack and streamflow composite records cover the 1951-2014 and 1909-2013  
268 periods, respectively (Fig. 2).

269  
270 The glacier mass balance reconstructions are based on simple linear regression models where the  
271 predictand is the 1975-2013 ECH annual mass balance series and the predictors are, alternatively,  
272 the regional 1951-2014 snowpack and 1909-2013 streamflow records depicted in Fig. 2. Given  
273 the relative shortness of the common period between the predictor and predictand series (39  
274 years), the reconstruction models were also developed using a “leave-one-out” cross-validation  
275 procedure (Michaelsen 1987). Here, linear regression models for each year were successively  
276 calibrated on the remaining 38 observations and then used to estimate the predictand’s value for  
277 the year omitted at each step. A simple linear regression model based on the full calibration  
278 dataset (1975-2013) was finally used to reconstruct the mass balance values over the complete  
279 period covered by the regional time series. The goodness of fit between observed and predicted  
280 mass balance values was tested based on the proportion of variance explained by the regression  
281 models and the normality, linear trend, and first- and higher-order autocorrelation of the  
282 regression residuals. The uncertainties in each reconstructed mass balance value in year  $t$  ( $\varepsilon_{reco,t}$ )  
283 were calculated integrating the standard error of the regression estimate ( $se_{regr}$ ) and the standard  
284 error of the mean annual streamflow values used as predictors in the model ( $se_{mean,t}$ ). This latter  
285 error is derived from the standard deviation of the regional record ( $\sigma$ ) and increases as the number  
286 of contributing streamflow series ( $n_t$ ) decreases back in time (see Table 3).

287

$$288 \varepsilon_{reco,t} = \sqrt{se_{regr}^2 + se_{mean,t}^2}, \text{ with} \quad (2)$$

289

$$290 se_{mean,t} = \frac{\sigma}{\sqrt{n_t}} \quad (3)$$

291

292 An independent verification of the reconstructed mass balance records was undertaken by  
293 comparing the cumulative patterns of these series with the cumulative mass balances reported for  
294 glaciario Piloto Este and for other glaciers with shorter mass balance series available in this portion  
295 of the Andes (Fig. 1A and Table 1). We also compared the ECH cumulative series (observed and  
296 predicted) with a regional record of glacier advances identified during the 20<sup>th</sup> century in the  
297 Andes between 29° and 35°S. The latter record was compiled in a recent review of glacier  
298 fluctuations in extratropical South America and is based on direct observations, reports from  
299 documentary evidence, and analyses of aerial photographs and satellite images from this region  
300 (see Masiokas et al. 2009). The uncertainty of the cumulative series modeled for ECH ( $\varepsilon_{cum,t}$ )  
301 were calculated by propagating (adding) the individual errors estimated for each reconstructed  
302 value. That is

303

304 
$$\varepsilon_{cum,t} = \sqrt{\varepsilon_{reco,t}^2 + \varepsilon_{reco,t+1}^2} \quad (4)$$

305

### 306 3 – Results

#### 307 3.1. Minimal glacier mass balance model

308 The 1975-2012 winter and summer values observed at ECH are depicted in Fig. 3A. The winter  
309 series shows a long term mean of 2.54 m w.eq. and a larger range of variability (std. dev. 1.24 m  
310 w.eq.) than the summer series, which fluctuates around a long term mean of -2.93 m w.eq (std.  
311 dev. 0.72 m w.eq.). The observed and modeled annual mass balance series are remarkably similar  
312 (Fig. 3B) and show a strong positive correlation ( $r = 0.883$ , rmse = 0.77 m w.eq.), indicating that  
313 78% of the variance in the ECH record can be accounted for by the minimal model presented in  
314 Eq. (1). Both series show similar, slightly negative linear trends and negative means (-0.35 and -  
315 0.34 m w.eq. for the observed and modeled series, respectively) over the 1977-2012 interval.

316

#### 317 3.2. Attribution assessments

318 In order to test which climate variable (temperature or precipitation) has a stronger influence on  
319 the annual mass balance variations at ECH, the glacier mass balance model was also run  
320 replacing alternatively the temperature and the precipitation monthly data by their long-term  
321 average values. The results from this analysis (Fig. 3C) suggest that precipitation variations  
322 constitute the dominant forcing modulating annual glacier mass balance at this site. Regardless of

323 their different absolute values, the precipitation-driven estimates (blue dashed line in Fig. 3C)  
324 show a strong positive correlation ( $r = 0.882$ ) and remarkable similarities with the ECH annual  
325 mass balance series (red line). In contrast, the temperature-driven estimates (dark red dashed line)  
326 show a poorer correlation with the ECH record ( $r = 0.240$ ) and a substantially lower inter-annual  
327 variability which only barely follows the variations in the annual mass balance series. To evaluate  
328 if the influence of temperature had been under-estimated in the full model (where the parameters  
329  $\alpha$  and  $\mu$  can compensate each other), both parameters were also optimized individually using a  
330 leave-one-out approach and considering each term of Eq. 1 as separate models. In this case the  
331 parameters showed almost exactly the same mean values (3.8 for  $\alpha$  and  $90.3 \text{ mm K}^{-1}$  for  $\mu$ ) as  
332 those obtained using the full model (3.9 and  $90.1 \text{ mm K}^{-1}$  for  $\alpha$  and  $\mu$ , respectively, see section  
333 2.2), suggesting that the poor performance of temperature is not due to the interaction of the  
334 parameters in the mass balance model.

335

### 336 **3.3 Annual mass balance reconstruction 1909-2013**

337 Fig. 4A shows the reconstruction of the ECH annual mass balance series based on the regional  
338 record of mean annual streamflows. The snowpack-based mass balance reconstruction is not  
339 shown as it is significantly shorter than the streamflow-based series and shows virtually the same  
340 variations over their overlapping interval. The streamflow-based regression model (Table 4) is  
341 able to explain 68% of the variance in the annual mass balance series over the 1975-2013 period  
342 and shows no apparent sign of model misspecification, offering the possibility of reliably  
343 extending the information on glacier mass balance changes back to 1909. This reconstructed  
344 mass balance record is almost three times longer than the mass balance record currently available  
345 at ECH and shows a strong year-to-year variability embedded within several periods of overall  
346 positive or negative conditions (Fig. 4A). In particular, positive mass balance conditions were  
347 reconstructed between 1914 and 1941, in the 1980s, and in the late 1990s – early 21st century. In  
348 contrast, the clearest sustained period of negative mass balances occurred between the 1940s and  
349 the 1970s.

350

351 The cumulative values of the streamflow-based mass balance reconstruction show a very good  
352 correspondence with the observed cumulative series and an overall negative trend between 1909  
353 and 2013 (Fig. 4B). Within this century-long negative trend, a prominent period of extended

354 positive mass balances can be observed between the mid 1910s and the early 1940s. After 1941  
355 and during the following four decades the cumulative mass balance series shows an impressive  
356 decline that is interrupted in 1980 by a ~10-year long period of sustained positive conditions (Fig.  
357 4B). Since the early 1990s and until 2013 the cumulative mass balance series resumes the  
358 negative tendency, only interrupted by a short-lived period of positive conditions in the first years  
359 of the 21<sup>st</sup> century. It is important to note, however, that ascribing absolute values to this  
360 reconstructed cumulative series is complicated and should be used with caution due to the large  
361 uncertainties involved, and the fact that the model is calibrated using reference-surface mass  
362 balance estimates (Cogley et al. 2011). Between 1975 and 2013 the lower elevation of the glacier  
363 did not change much (see Fig. 1C) and therefore the reference-surface and the conventional mass  
364 balance estimates are probably roughly equivalent. However, for earlier decades and without  
365 historical information on the glacier area and frontal position, it is difficult to estimate the  
366 impacts of changing glacier geometry on the actual mass balance of this glacier.

367

### 368 **3.4 Comparison with other glacier records**

369 Examination of the main patterns in the reconstructed cumulative mass balance series shows a  
370 good correspondence with a regional record of glacier advances identified in the Central Andes  
371 over the past 100 years (Masiokas et al. 2009; Fig. 4C). In most cases, the glacier advances are  
372 concentrated during, or soon after, the periods of sustained positive mass balances reconstructed  
373 or observed at ECH. This situation is particularly clear in the 1980s and 1990s, where a large  
374 number of glacier advances were identified during and/or immediately after the peak in mass  
375 balances that culminated in 1989 (Fig. 4BC). Glacier advances were also identified in the 1930s,  
376 1940s and 1950s likely associated with the extended period of cumulative positive mass balances  
377 that culminated in the early 1940s. A few well documented advances identified in this region  
378 between 2003 and 2007 may be associated with the minor peak in cumulated mass balances  
379 observed at the turn of the 21<sup>st</sup> century (Fig. 4BC).

380

381 The cumulative variations in the modeled and observed mass balance series from ECH are also  
382 very similar to those observed in the 1979-2002 cumulative record of PIL, providing additional  
383 support for the overall reliability of the reconstructed time series (Fig. 5). The cumulative  
384 tendency of PIL appears to be “smoother” than the ECH series, but still shows slightly positive or

385 near equilibrium conditions between the late 1970s and the mid 1980s followed by a sharp  
386 decline until the turn of the 21<sup>st</sup> century. The cumulative series from other glaciers located further  
387 north in the Pascua Lama and Cordillera de Colanguil areas (Fig. 1A and Table 1) only cover the  
388 last decade or so of the ECH record. However, in all cases their overall tendency is similar and  
389 markedly negative, reflecting the sustained unfavorable conditions that these ice masses have  
390 endured in recent years. It is interesting to note that the smaller glaciers (Table 1 and Fig. 5) are  
391 the ones consistently showing the steepest negative cumulative trends whereas the largest glacier  
392 (glaciar Guanaco, with ca. 1.8 km<sup>2</sup> in 2007) shows the least negative trend.

393

#### 394 **4 – Discussion and Conclusions**

395 Compared to other mountainous glacierized areas, the extratropical Andes in southern South  
396 America contain one of the least complete networks of *in situ* glacier mass balance and high-  
397 elevation climate records in the world. This scarcity of basic information in this extensive and  
398 glaciologically diverse region has been highlighted on many occasions, and several recent studies  
399 have attempted to overcome this limitation by estimating mass balance changes through remote  
400 sensing and/or modeling approaches of varied complexity and spatial coverage (e.g. Casassa et  
401 al. 2006; Radić et al. 2013; Lenaerts et al. 2014; Pellicciotti et al. 2014; Schaefer et al. 2013,  
402 2015). With such limited data availability, the few existing glacier mass balance records become  
403 particularly relevant as they provide crucial information and validation measures for many  
404 glaciological, climatological and hydrological analyses.

405

406 In this paper we analyzed an up-to-date compilation of the longest and most complete *in situ*  
407 glacier mass balance and hydro-climatic records from the Andes between 29° and 37°S to address  
408 some basic (yet poorly known) glaciological issues in this region. First, we show that it is  
409 possible to estimate annual glacier mass balance changes using very simple modeling approaches.  
410 Results from a minimal model requiring only monthly temperature and precipitation data (eq. 1)  
411 revealed that up to 78% of the variance in the annual mass balance series between 1977 and 2012  
412 could be captured simply using available records from the El Yeso station, ca. 10 km from the  
413 glacier (Fig. 1A and 3B). Winter precipitation variability appears to be the dominant forcing  
414 modulating annual mass balances at ECH, with temperature variations likely playing a secondary  
415 role (Fig. 3C). This is particularly interesting because it contrasts with the findings in other

416 regions where the recent glacier behavior is generally more strongly related to changes in  
417 temperature instead of precipitation (e.g. Marzeion et al. 2012). However, and although Peña and  
418 Narbona (1978) also noted a dominant influence of the winter accumulation term on the resulting  
419 annual mass balance of this glacier, the results should be assessed with caution given the  
420 simplistic nature of our model and the various factors that ultimately affect the annual mass  
421 balance at this site. For example, more detailed assessments should also consider the impact of  
422 sublimation on the mass balance of glaciers in this high arid portion of the Andes (McDonell et  
423 al. 2013; Pellicciotti et al. 2014).

424

425 To test the reliability of the temperature records used to model the glacier mass balance series we  
426 correlated the El Yeso monthly temperature record with ERA Interim gridded reanalysis  
427 temperatures for the 700 mb geopotential height (roughly 3000 m asl), and also with a 0°C  
428 isotherm elevation series available from central Chile (Fig. 6). The El Yeso temperature record  
429 shows strong positive correlations with ERA Interim gridded data over an extensive region that  
430 includes central Argentina, central Chile and an adjacent area in the Pacific Ocean (Fig. 6A). The  
431 El Yeso temperature record also shows clear similarities and a positive significant correlation  
432 with the 0°C isotherm elevation series over the 1977-2004 interval (Fig. 6B-C). The  
433 independence of these three datasets indicates that the El Yeso mean monthly temperature data  
434 are reliable and that the poor performance of this variable in the mass balance modeling exercise  
435 is not related to the overall quality of the temperature series. Although this issue is beyond the  
436 main purposes of this study, more complex modeling approaches are also needed to evaluate if  
437 climate data at higher temporal resolution (instead of monthly values as used here) are capable of  
438 capturing a larger percentage of the mass balance variations observed at ECH.

439

440 Annual mass balance variations observed at ECH can also be reproduced or estimated accurately  
441 through simple linear regression using regionally-averaged winter snowpack or annual  
442 streamflow records as predictors (Fig. 4A). This is due to the existence of a strong common  
443 hydroclimatic signal in this region, which results in very similar inter-annual variations in winter  
444 snow accumulation, mean annual river discharges, and glacier mass balance changes such as  
445 those measured at ECH (Fig. 2). This simple approach allows extending the information on  
446 glacier mass balance changes several decades prior to the beginning of in situ measurements

447 (back to 1909), and offers the opportunity of putting the existing glacier record in a longer term  
448 perspective. Many of the extreme values reconstructed in this study have been documented in  
449 historical reports and recent analyses of instrumental hydro-climatic data. For example, the  
450 extreme positive values of 1914 and 1919 coincide with extremely wet winters in central Chile  
451 (see e.g. Fig. 2; Taulis 1934; Masiokas et al. 2012), whereas the period with above average  
452 balances centered in the 1980s or the negative conditions between the 1940s and 1970s have been  
453 identified, respectively, as the snowiest and driest intervals during the instrumental era in this  
454 region (Masiokas et al. 2010). Examination of the main intra- to multi-decadal patterns in this  
455 extended series also indicates that the sustained negative mass balance conditions reported for  
456 ECH in recent years are not unusual and were probably surpassed by more negative and longer  
457 periods between the 1940s and 1970s (Fig. 4A). However, the impact of a few consecutive years  
458 of negative mass balances are more serious today than several decades ago because of the low  
459 volume of ice remaining and the poorer overall “health” of the glacier.

460  
461 The cumulative series of the reconstructed mass balances values (Fig. 4B) shows a steep negative  
462 trend that is consistent with the recent loss of ice reported for other glaciers in this region (Fig. 5;  
463 Escobar et al. 1995; Rivera et al. 2000; Masiokas et al. 2009). This negative trend has been  
464 temporarily interrupted by periods of sustained positive mass balances that, in most cases,  
465 precede or coincide with recent glacier re-advances identified at these latitudes in the Andes  
466 (Masiokas et al. 2009; Fig. 4C). The clearest example is the relationship between the peak in  
467 cumulative mass balances in the mid-late 1980s and the 11 documented glacier advances in the  
468 following decade. It is also interesting to note that several of the glacier events that occurred after  
469 periods of positive mass balances have been identified as surges (Helbling 1935; Espizua 1986;  
470 Masiokas et al. 2009; Pitte et al. 2016). The well-known surges of Grande del Nevado glacier (in  
471 the Plomo massif area) in 1933-34, 1984-85, and 2004-2007 are particularly noteworthy as they  
472 consistently occurred near the culmination of the three periods with overall positive mass  
473 balances in the 1920s-30s, in the 1980s and in the first decade of the 21<sup>st</sup> century (Fig. 4B). In  
474 agreement with the progressively smaller magnitude of these peaks in the cumulative mass  
475 balance series, the three Grande del Nevado surges also showed a decreasing power and  
476 transferred progressively smaller quantities of mass from the upper to the lower parts of the  
477 glacier. Two recent surges of Horcones Inferior glacier in the nearby Mt. Aconcagua area also

478 occurred in the mid 1980s and again between 2002 and 2006, suggesting a possible connection  
479 between the development of surging events and the periods with overall positive mass balance  
480 conditions in this region (Pitte et al. 2016).

481  
482 The fact that only limited information is available for ECH together with the use of reference-  
483 surface mass balance estimates (see section 2.1) pose interesting yet complicated questions  
484 regarding the applicability of this series in related glaciological and/or climatological  
485 assessments. Since reference-surface mass balance variations are more closely related to changes  
486 in climate than the conventional mass balance of a glacier (Cogley et al. 2011), the reconstructed  
487 series discussed here is arguably more relevant to climate-change related studies rather than  
488 hydrological studies. If the purpose is to evaluate the hydrological contribution of this ice mass  
489 over the last century, then conventional mass balance estimates are necessarily required to take  
490 the changing glacier geometry into account. In any case, and considering the relevance of the  
491 observed ECH series for regional, hemispheric and global mass balance studies, a reanalysis  
492 (Zemp et al. 2013) of the entire mass balance record would probably produce important  
493 worthwhile information to properly assess the hydrological impact of the recent ice mass losses  
494 in this semi-arid region (e.g. Ragettli et al. 2014). This issue is particularly relevant due to the  
495 extended droughts experienced in recent years and the increasing socio-economic conflicts over  
496 the limited water resources (almost entirely originating in the mountains) arising on both sides of  
497 the Andes.

498  
499 Keeping these caveats in mind, the common pattern of strongly negative mass balances, the  
500 similarities with the few available glacier chronologies, and the regional nature of the predictors  
501 used in the ECH reconstruction suggest that this series may nonetheless be considered  
502 representative (in relative terms) of the mass balance changes during recent decades in other less  
503 studied areas in this region. Reliable data from a larger number of glaciers together with  
504 additional studies of the glacier-climate relationships are, however, still needed to support this  
505 hypothesis and to identify, for example, the main climatic forcings behind the recent glacier  
506 shrinkage observed in the Central Andes of Chile and Argentina (Masiokas et al. 2009). This is a  
507 challenging issue due to several factors, including the serious lack of glacier mass balance series  
508 and high-elevation climate records, the complex dynamic response of individual glaciers to

509 similar changes in climate, and the great variety of glaciers existing in this region (Pellicciotti et  
510 al. 2014). The results discussed in this study offer a useful starting point to address the various  
511 pending issues mentioned above and will hopefully stimulate further glaciological, climatological  
512 and hydrological research in this poorly known mountainous region.

513

## 514 **6 – Acknowledgements**

515 This work was funded by Consejo Nacional de Investigaciones Científicas y Técnicas  
516 (CONICET, Argentina), FONDECYT Grant 1121106, and FONDAP Grant 15110009 (Chile).  
517 We greatly acknowledge the World Glacier Monitoring Service (<http://www.wgms.ch>),  
518 Dirección General de Aguas (<http://www.dga.cl>), Dirección Meteorológica de Chile  
519 (<http://www.meteochile.gob.cl>), and Subsecretaría de Recursos Hídricos  
520 (<http://www.hidricosargentina.gov.ar>) for providing the data used in this study. ERA-Interim  
521 reanalysis data and correlation maps were provided by the freely available Climate Explorer  
522 online application maintained by Geert Jan van Oldenborgh at the Royal Netherlands  
523 Meteorological Institute (KNMI; <http://climexp.knmi.nl/>). E. Berthier acknowledges support  
524 from the French Space Agency (CNES) through his TOSCA program, S.U. Nussbaumer  
525 acknowledges support from the Swiss National Science Foundation (project PBBEP2-139400),  
526 and A. González-Reyes acknowledges the support from CONICYT (Chile) to conduct his PhD  
527 studies. The comments and suggestions from the handling Editor and three anonymous reviewers  
528 significantly improved the manuscript and are greatly appreciated.

529 **7 – References**

530

531 Aceituno, P. (1988), On the functioning of the Southern Oscillation in the South American sector.  
532 Part I: Surface climate, *Mon. Weather Rev.*, 116, 505– 524.

533 Casassa, G., Rivera, A. and Schwikowski, M. 2006. Glacier mass-balance data for southern South  
534 America (30°S-56°S). In: *Glacier Science and Environmental Change* (ed P. G. Knight),  
535 Blackwell Publishing, Malden, MA, USA. doi: 10.1002/9780470750636.ch47

536 Cara, L., M. Masiokas, M. Viale, R. Villalba (in press). Assessing snow cover variations in the  
537 Río Mendoza upper basin using MODIS satellite imagery. *Revista Meteorológica*, 25 p.  
538 (in Spanish).

539 Cogley, J.G., R. Hock, L.A. Rasmussen, A.A. Arendt, A. Bauder, R.J. Braithwaite, P. Jansson, G.  
540 Kaser, M. Möller, L. Nicholson and M. Zemp, 2011, *Glossary of Glacier Mass Balance*  
541 and Related Terms, IHP-VII Technical Documents in Hydrology No. 86, IACS  
542 Contribution No. 2, UNESCO-IHP, Paris.

543 DGA. 2009. Radio Eco-sondaje en la cuenca del río Maipo y mediciones glaciológicas en el  
544 glaciar Tyndall, Campo de Hielo Sur. Dirección General de Aguas, Santiago de Chile,  
545 S.I.T. 204, 95 pp.

546 DGA, 2010. Balance de masa en el glaciar Echaurren Norte temporadas 1997-1998 a 2008-2009.  
547 Dirección General de Aguas, Santiago de Chile, 32 pp.

548 Escobar, F., Casassa G, Pozo V. 1995a. Variaciones de un glaciar de montaña en los Andes de  
549 Chile central en las últimas dos décadas. *Bull Inst Fr Etud Andin* 1995;24(3):683–95.

550 Escobar, F., Pozo, V., Salazar, A., y Oyarzo, M., 1995b. Balance de masa en el glaciar Echaurren  
551 Norte, 1975 a 1992. Resultados preliminares. Dirección General de Aguas. (Publicación  
552 DGA, H.A. y G. 95/1), 106 p.

553 Escobar, F. and Garín, C. 1997. Complemento N° 1, años 1993-1996, al “Balance de masa en el  
554 glaciar Echaurren Norte, 1975 a 1992. Resultados preliminares”. Dirección General de  
555 Aguas. (Publicación DGA, H.A. y G. 97/1), 18 p.

556 Espizua, L. 1986. Fluctuations of the Río del Plomo Glaciers. *Geografiska Annaler*, 68A(4): 317-  
557 327.

558 Falvey, M.; Garreaud, R.D. 2009. Regional cooling in a warming world: Recent temperature  
559 trends in the southeast Pacific and along the west coast of subtropical South America

560 (1979–2006). *Journal of Geophysical Research* 114, D04102,  
561 doi:10.1029/2008JD010519.

562 Garreaud, R.D. 2009. The Andes climate and weather. *Advances in Geosciences* 7, 1–9.

563 Helbling, R. 1935. The origin of the Río Plomo ice-dam. *The Geographical Journal*, 8(1): 41-49.

564 Kaser, G., Grosshauser, M., and Marzeion, B.: Contribution potential of glaciers to water  
565 availability in different climate regimes, *P. Natl. Acad. Sci. USA*, 107, 20223–20227,  
566 doi:10.1073/pnas.1008162107, 2010.

567 Le Quesne, C., et al. (2009), Long-term glacier variations in the Central Andes of Argentina and  
568 Chile, inferred from historical records and tree-ring reconstructed precipitation,  
569 *Palaeogeogr. Palaeoclimatol. Palaeoecol.*, 281, 334-344.

570 Leiva, J.C.; Cabrera, G.A.; Lenzano, L.E. 2007. 20 years of mass balances on the Piloto glacier,  
571 Las Cuevas river basin, Mendoza, Argentina. *Global and Planetary Change* 59, 10–16.

572 Lenaerts, J.T.M., M.R. van den Broeke, J.M. van Wessem, W.J. van de Berg, E. van Meijgaard,  
573 L.H. van Ulft, and M. Schaefer. 2014. Extreme precipitation and climate gradients in  
574 Patagonia revealed by high-resolution regional atmospheric climate modeling. *Journal of  
575 Climate* 27, 4607–4621.

576 Lliboutry, L., 1998: Glaciers of the dry Andes. *Satellite Image Atlas of Glaciers of the World:*  
577 *South America*, R. S. Williams and J. G. Ferrigno, Eds., USGS Professional Paper 1386-I.  
578 Available online at <http://pubs.usgs.gov/prof/p1386i/index.html>.

579 MacDonell, S., C. Kinnard, T. Mölg, L. Nicholson, and J. Abermann. 2013. Meteorological  
580 drivers of ablation processes on a cold glacier in the semi-arid Andes of Chile. *The  
581 Cryosphere*, 7, 1513–1526, doi:10.5194/tc-7-1513-2013

582

583 Marzeion, B., M. Hofer, A. H. Jarosch, G. Kaser, and T. Molg. 2012. A minimal model for  
584 reconstructing interannual mass balance variability of glaciers in the European Alps. *The  
585 Cryosphere*, 6, 71–84, doi:10.5194/tc-6-71-2012.

586 Masiokas, M.H.; Villalba, R.; Luckman, B.; LeQuesne, C.; Aravena, J.C. 2006. Snowpack  
587 variations in the central Andes of Argentina and Chile, 1951-2005: Large-scale  
588 atmospheric influences and implications for water resources in the region. *Journal of  
589 Climate* 19 (24), 6334-6352.

590 Masiokas, M.H.; Villalba, R.; Luckman, B.; Delgado, S.; Lascano, M.; Stepanek, P. 2008. 20th-  
591 century glacier recession and regional hydroclimatic changes in northwestern Patagonia.  
592 *Global and Planetary Change* 60 (1-2), 85-100.

593 Masiokas, M.H.; Rivera, A.; Espizua, L.E.; Villalba, R.; Delgado, S.; Aravena, J.C. 2009. Glacier  
594 fluctuations in extratropical South America during the past 1000 years. *Palaeogeography,*  
595 *Palaeoclimatology, Palaeoecology* 281 (3-4), 242-268.

596 Masiokas, M.H.; Villalba, R.; Luckman, B.H.; Mauget, S. 2010. Intra- to multidecadal variations  
597 of snowpack and streamflow records in the Andes of Chile and Argentina between 30°  
598 and 37°S. *Journal of Hydrometeorology* 11 (3), 822-831.

599 Masiokas, M.H.; Villalba, R.; Christie, D.A.; Betman, E.; Luckman, B.H.; Le Quesne, C.; Prieto,  
600 M.R.; Mauget, S. 2012. Snowpack variations since AD 1150 in the Andes of Chile and  
601 Argentina (30°-37°S) inferred from rainfall, tree-ring and documentary records. *Journal of*  
602 *Geophysical Research - Atmospheres*, 117, D05112, doi:10.1029/2011JD016748.

603 Miller, A., 1976: The climate of Chile. *World Survey of Climatology*. W. Schwerdtfeger, Ed.,  
604 Vol. 12, Elsevier, 113–218.

605 Pellicciotti, F.; Ragettli, S.; Carenzo, M.; McPhee, J. 2014. Changes of glaciers in the Andes of  
606 Chile and priorities for future work. *Science of the Total Environment* 493, 1197–1210.

607 Peña, H.; Narbona, J. 1978. Proyecto Glaciar Echaurren Norte, Informe preliminar. Dirección  
608 General de Aguas, Departamento de Hidrología (in Spanish). 75 p.

609 Pitte, P.; Berthier, E.; Masiokas, M.H.; Cabot, V.; Ruiz, L.; Ferri Hidalgo, L.; Gargantini, H.;  
610 Zalazar, L. 2016. Geometric evolution of the Horcones Inferior Glacier (Mount  
611 Aconcagua, Central Andes) during the 2002–2006 surge. *Journal of Geophysical*  
612 *Research, Earth Surface*, 121, 111–127, doi:10.1002/2015JF003522.

613 Popovnin, V.V., Danilova, T.A., Petrakov, D.A., 1999. A pioneer mass balance estimate for a  
614 Patagonian glacier: Glaciar De los Tres, Argentina. *Global and Planetary Change* 22 (1),  
615 255–267.

616 Rabatel, A.; H. Catebrunet, V. Favier, L. Nicholson, C. Kinnard. 2011. Glacier changes in the  
617 Pascua Lama region, Chilean Andes (29 S): recent mass balance and 50 years surface area  
618 variations. *The Cryosphere* 5, 1029–1041.

619 Radić, V.; Bliss, A.; Beedlow, A.C.; Hock, R.; Miles, E.; Cogley, J.G.; Regional and global  
620 projections of twenty-first century glacier mass changes in response to climate scenarios  
621 from global climate models. *Climate Dynamics*, DOI 10.1007/s00382-013-1719-7

622 Ragettli S., Cortés G., McPhee J., Pellicciotti F. 2014. An evaluation of approaches for modelling  
623 hydrological processes in high-elevation, glacierized Andean watersheds, *Hydrological  
624 Processes* 28, 5674–5695, doi: 10.1002/hyp.10055

625 Rignot, E., A. Rivera, G. Cassasa. 2003. Contribution of the Patagonia Icefields to sea level rise.  
626 *Science* 302, 434-437.

627 Rasmussen, L., Conway, H., Raymond, C., 2007. Influence of upper air conditions on the  
628 Patagonia Icefields. *Global and Planetary Change* 59, 203–216.

629 Rivera, A., G. Casassa, C. Acuña, and H. Lange, 2000: Recent glacier variations in Chile (in  
630 Spanish). *Investigaciones Geográficas* 34, 29–60.

631 Rivera, A.; Bown, F; Casassa, G.; Acuña, C.; Clavero, J. 2005. Glacier shrinkage and negative  
632 mass balance in the Chilean Lake District (40°S). *Hydrological Sciences Journal*, 50(6):  
633 963-974.

634 Ruiz, L.; Pitte, P.; Masiokas, M. 2013. The initiation of mass balance studies on the Argentinean  
635 glaciers on Mount Tronador. CRN2047 Science Meeting, Uspallata, Argentina, April 21-  
636 25, 2013.

637 Schaefer, M., Machguth, H., Falvey, M., Casassa, G. 2013. Modeling past and future surface  
638 mass balance of the Northern Patagonia Icefield. *J. Geophys. Res.*, 118, 571–588, doi:  
639 10.1002/jgrf.20038.

640 Schaefer M., Machguth H., Falvey M., Casassa G., Rignot E. 2015. Quantifying mass balance  
641 processes on the Southern Patagonia Icefield. *Cryosphere*, 9(1), 25–35, doi: 10.5194/tc-9-  
642 25-2015.

643 Taulis, E. 1934. De la distribucion de pluies au Chili. *Matér. Étude Calamités*, 33, 3-20.

644 Villalba, R.; Lara, A.; Boninsegna, J.A.; Masiokas, M.H.; Delgado, S.; Aravena, J.C.; Roig, F.;  
645 Schmelter, A.; Wolodarsky, A.; Ripalta, A. 2003. Large-scale temperature changes across  
646 the southern Andes: 20th-century variations in the context of the past 400 years. *Climatic  
647 Change* 59 (1-2), 177-232.

648 WGMS. 2013. Glacier Mass Balance Bulletin No. 12 (2010-2011). Zemp, M., Nussbaumer, S.U.,  
649 Naegeli, K., Gärtner-Roer, I., Paul, F., Hoelzle, M., and Haeberli, W. (eds.), ICSU (WDS)

650 / IUGG (IACS) / UNEP / UNESCO / WMO, World Glacier Monitoring Service, Zurich,  
651 Switzerland: 106 pp., publication based on database version: doi: 10.5904/wgms-fog-  
652 2013-11.  
653 Zemp, M., E. Thibert, M. Huss, D. Stumm, C. Rolstad Denby, C. Nuth, S.U. Nussbaumer, G.  
654 Moholdt, A. Mercer, C. Mayer, P. C. Joerg, P. Jansson, B. Hynek, A. Fischer, H. Escher-  
655 Vetter, H. Elvehøy, and L. M. Andreassen. 2013. Reanalysing glacier mass balance  
656 measurement series. *The Cryosphere*, 7, 1227–1245, doi:10.5194/tc-7-1227-2013  
657  
658

659 **Table 1.** Basic information of the glacier mass balance series used in this study. (\*) Country: CL:  
 660 Chile; AR: Argentina.

Name	ID in Fig. 1	Lat., Long.	Area in km <sup>2</sup> (year)	Period	Ctry*	References
Echaurren Norte	ECH	33°33'S, 70°08'W	0.226 (2008)	1975-2013	CL	DGA 2009; Baraza (DGA); WGMS 2013
Piloto Este	PIL	32°13'S, 70°03'W	0.504 (2007)	1979-2002	AR	Leiva et al. 2007; WGMS 2013
Conconta Norte	COL	29°58'S, 69°39'W	0.089 (2012)	2008-2013	AR	Cabrera and Leiva (IANIGLA); WGMS 2013
Brown Superior	COL	29°59'S, 69°38'W	0.191 (2012)	2008-2013	AR	Cabrera and Leiva (IANIGLA); WGMS 2013
Los Amarillos	COL	29°18'S, 69°59'W	0.954 (2012)	2008-2013	AR	Cabrera and Leiva (IANIGLA); WGMS 2013
Amarillo	PAS	29°18'S, 70°00'W	0.243 (2012)	2008-2013	CL	Cabrera and Leiva (IANIGLA); WGMS 2013
Toro 1	PAS	29°20'S, 70°01'W	0.071 (2007)	2004-2009	CL	Rabatel et al. 2011; WGMS 2013
Toro 2	PAS	29°20'S, 70°01'W	0.066 (2007)	2004-2009	CL	Rabatel et al. 2011; WGMS 2013
Esperanza	PAS	29°20'S, 70°02'W	0.041 (2007)	2004-2009	CL	Rabatel et al. 2011; WGMS 2013
Guanaco	PAS	29°19'S, 70°00'W	1.836 (2007)	2004-2013	CL/ AR	Rabatel et al. 2011; Rivera (CECs); WGMS 2013

661

662

663 **Table 2.** Correlation analyses between the ECH mass balance series and regional hydro-climatic  
664 records. The number of observations used in each correlation test is indicated in parenthesis.  
665 Note: \* (\*\*) Pearson correlation coefficient is significant at the 95% (99%) confidence level.

666

	Winter ECH	Annual mass balance ECH	Regional snowpack	Regional streamflow
Summer ECH	0.245 (38)	0.648 ** (38)	0.447 ** (38)	0.395 * (38)
Winter ECH		0.897 ** (38)	0.796 ** (38)	0.834 ** (38)
Annual mass balance ECH			0.829 ** (39)	0.826 ** (39)
Regional snowpack				0.916 ** (63)

667

668

669

670      **Table 3.** Stations used to develop regionally-averaged series of mean annual river discharges and  
 671      winter maximum snow accumulation for the Andes between 30° and 37°S. Mean annual  
 672      streamflow values refer to a July-June water year. Note: (\*) The 1981-2010 climatology values  
 673      for each station are expressed as mm w.eq. for snowpack and as  $m^3 s^{-1}$  for streamflow. In the case  
 674      of the San Juan and Cachapoal rivers, the mean values used correspond to the 1981-2007 and  
 675      1981-2001 periods, respectively. Data sources: (DGA) Dirección General de Aguas, Chile; (DGI)  
 676      Departamento General de Irrigación, Mendoza, Argentina; (SSRH) Subsecretaría de Recursos  
 677      Hídricos, Argentina. See Masiokas et al. (2013) for further details.  
 678

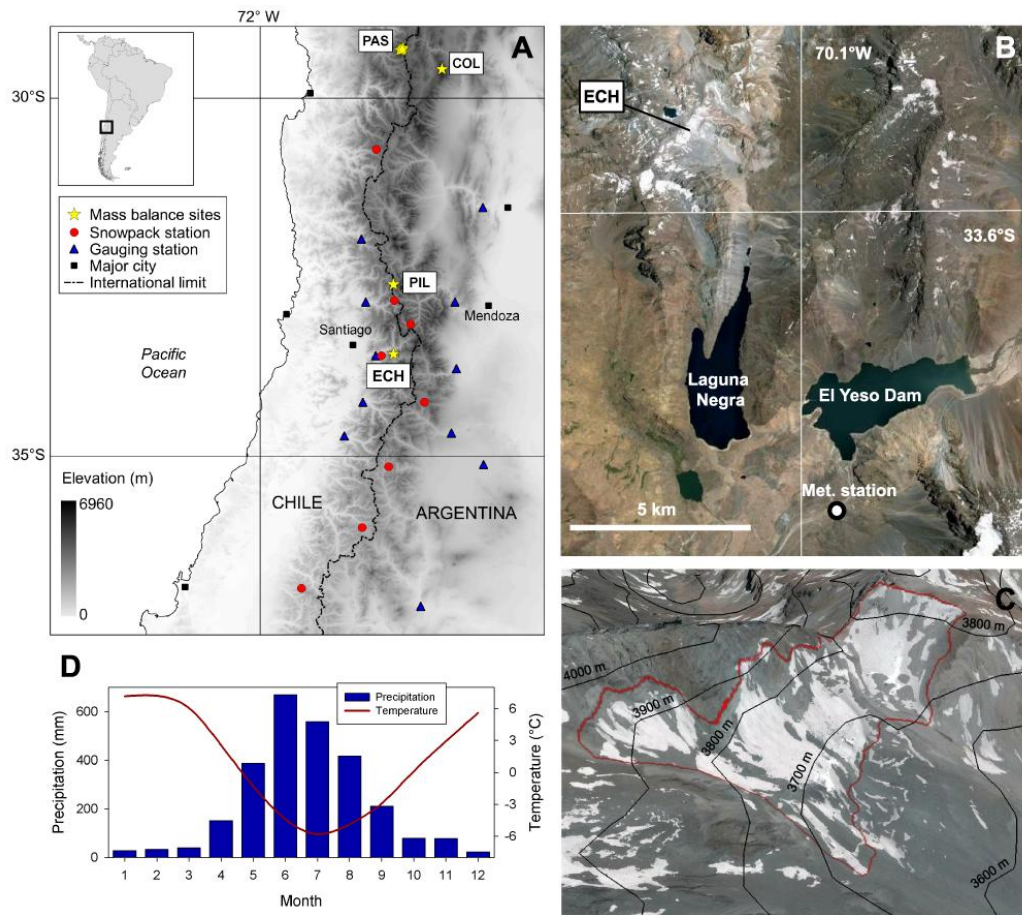
Variable	Station	Lat., Long.	Elev.	Period	1981-2010 mean*	Data source
A - Snowpack	Quebrada Larga	30°43'S, 70°22'W	3500 m	1956-2014	273	DGA
	Portillo	32°50'S, 70°07'W	3000 m	1951-2014	703	DGA
	Toscas	33°10'S, 69°53'W	3000 m	1951-2014	354	DGI
	Laguna Negra	33°40'S, 70°08'W	2768 m	1965-2014	632	DGA
	Laguna del Diamante	34°15'S, 69°42'W	3310 m	1956-2014	472	DGI
	Valle Hermoso	35°09'S, 70°12'W	2275 m	1952-2014	756	DGI
	Lo Aguirre	36°00'S, 70°34'W	2000 m	1954-2014	934	DGA
	Volcán Chillán	36°50'S, 71°25'W	2400 m	1966-2014	757	DGA
B - Streamflow (river)	Km. 47.3 (San Juan)	31°32'S 68°53'W	945 m	1909- 2007	68.2	SSRH
	Guido (Mendoza)	32°51'S 69°16'W	1550 m	1909-2013	52.4	SSRH
	Valle de Uco (Tunuyán)	33°47'S 69°15'W	1200 m	1954-2013	30.6	SSRH
	La Jaula (Diamante)	34°40'S 69°19'W	1500 m	1938-2013	35.6	SSRH
	La Angostura (Atuel)	35°06'S 68°52'W	1200 m	1948-2013	39.1	SSRH
	Buta Ranquil (Colorado)	37°05'S 69°44'W	850 m	1940-2013	154.8	SSRH
	Cuncumén (Choapa)	31°58'S 70°35'W	955 m	1941-2013	10.3	DGA
	Chacabuquito (Aconcagua)	32°51'S 70°31'W	1030 m	1914-2013	34.7	DGA
	El Manzano (Maipo)	33°36'S 70°23'W	890 m	1947-2013	123.0	DGA
	Termas de Cauquenes (Cachapoal)	34°15'S 70°34'W	700 m	1941-2001	93.6	DGA
	Bajo Los Briones (Tinguiririca)	34°43'S 70°49'W	518 m	1942-2013	53.8	DGA

681 **Table 4.** Summary statistics for the simple linear regression models used to estimate ECH annual  
 682 mass balances using regional snowpack and streamflow records. Notes: (adj  $r^2$ ) adjusted  
 683 coefficient of determination used to estimate the proportion of variance explained by regression;  
 684 (F) F-ratio for ANOVA test of the null hypothesis that all model coefficients are 0; (Se) standard  
 685 error of the estimate; (rmse) root-mean-squared error of regression. (b0) constant of regression  
 686 model; (b1) regression coefficient; (DWd) Durbin-Watson d statistic used to test for first-order  
 687 autocorrelation of the regression residuals. (Port. Q) Portmanteau Q statistic to test if high-order  
 688 autocorrelation in the regression residuals is different from 0. (ns) results are not statistically  
 689 significant at the 95% confidence level; (\*\*) statistically significant at the 99% confidence level.  
 690

Predictor	Model statistics						Residual statistics		
	Adj $r^2$	F	Se	rmse	b0 (std. error)	b1 (std. error)	Slope	DWd	Port. Q
<b>Snowpack</b>	0.686	80.99**	0.889	0.911	-2.899 (0.316)**	0.026 (0.003)**	-0.003ns	2.2ns	5.7ns
<b>Streamflow</b>	0.682	79.49**	0.894	0.919	-4.045 (0.439)**	0.038 (0.004)**	0.006ns	2.3ns	4.9ns

691

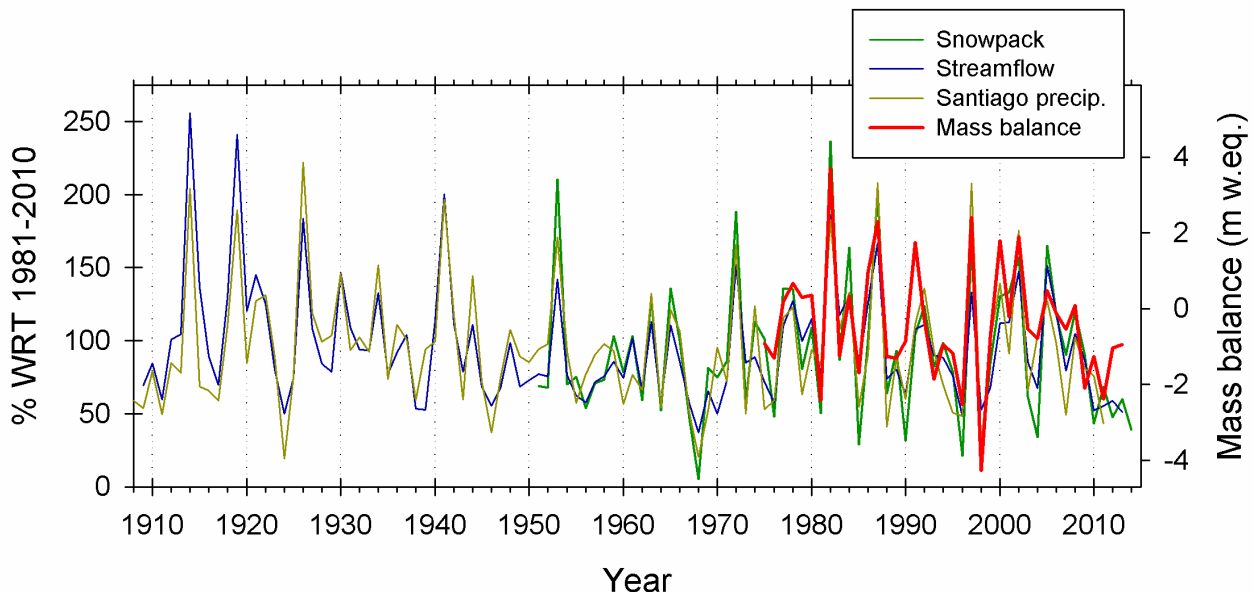
692



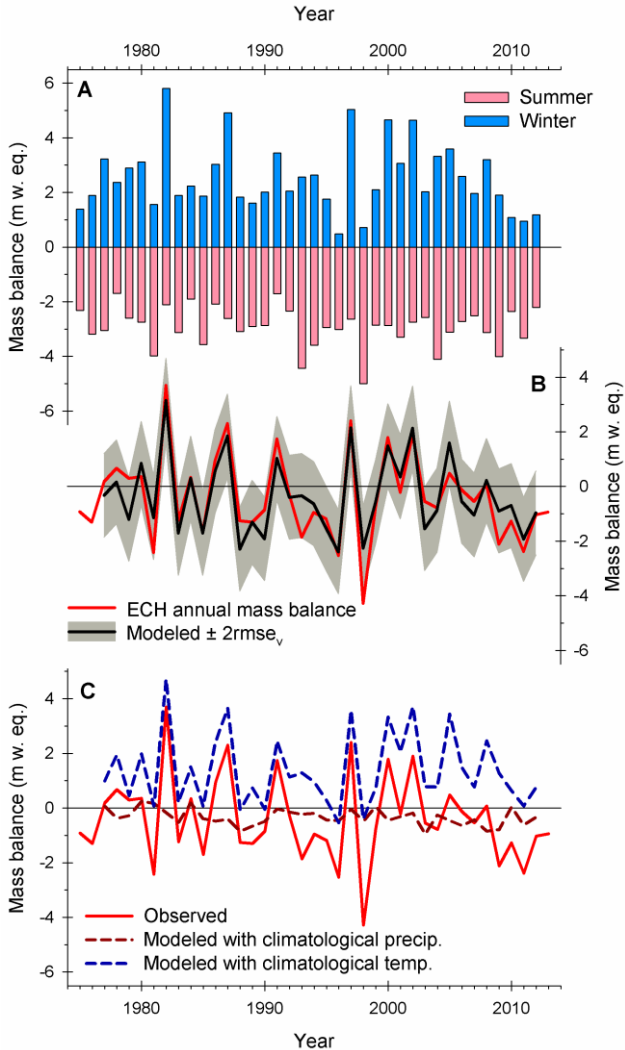
693

694 **Figure 1.** **A)** Map of the Central Andes of Chile and Argentina showing the location of glacier  
 695 Echaurren Norte (ECH), glacier Piloto Este (PIL), and several smaller glaciers with mass balance  
 696 records in the Pascua Lama (PAS) and Cordillera de Colanguil (COL) areas. The locations of the  
 697 snowpack and streamflow stations discussed in the text are also shown (Tables 1 and 2). **B)**  
 698 General view of the El Yeso area, showing the location of ECH, El Yeso Dam, and the associated  
 699 meteorological station. Laguna Negra is a natural lake that receives the meltwater from ECH.  
 700 Base image acquired on January 5, 2014 and downloaded from Google Earth. **C)** Closer 3D view  
 701 of glacier Echaurren Norte as observed in 2014 and in the early 1970s (outlined in red and based  
 702 on Peña and Narbona 1978). Note that the glacier has remained in roughly the same position but  
 703 has thinned markedly over the last decades. **D)** Seasonal variations in temperature and  
 704 precipitation at the lower reaches of ECH (3700 m asl) extrapolated from the El Yeso  
 705 meteorological station (see section 2.2 for details). Note that the bulk of precipitation occurs  
 706 during the coldest months of the year (December-March precipitation only accounts for ~5% of  
 707 the mean annual totals).

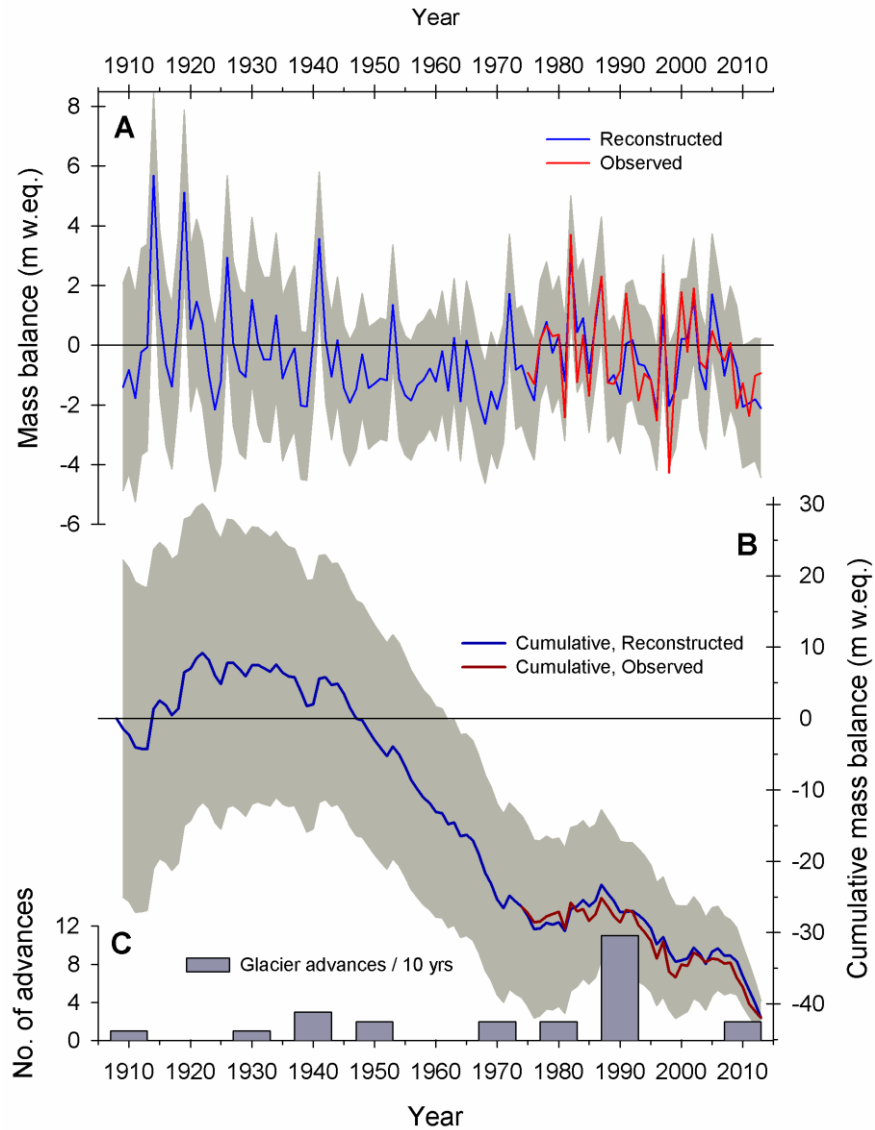
708



709  
710 **Figure 2.** Comparison between the annual mass balance series of ECH and regional records of  
711 maximum winter snow accumulation and mean annual river discharges in the Andes between 30°  
712 and 37°S (see Fig. 1). The regional records are expressed as percentages with respect to the 1981-  
713 2010 mean values. Variations in annual total precipitation at Santiago are also included to  
714 highlight the strong hydro-climatic signal in this region.  
715



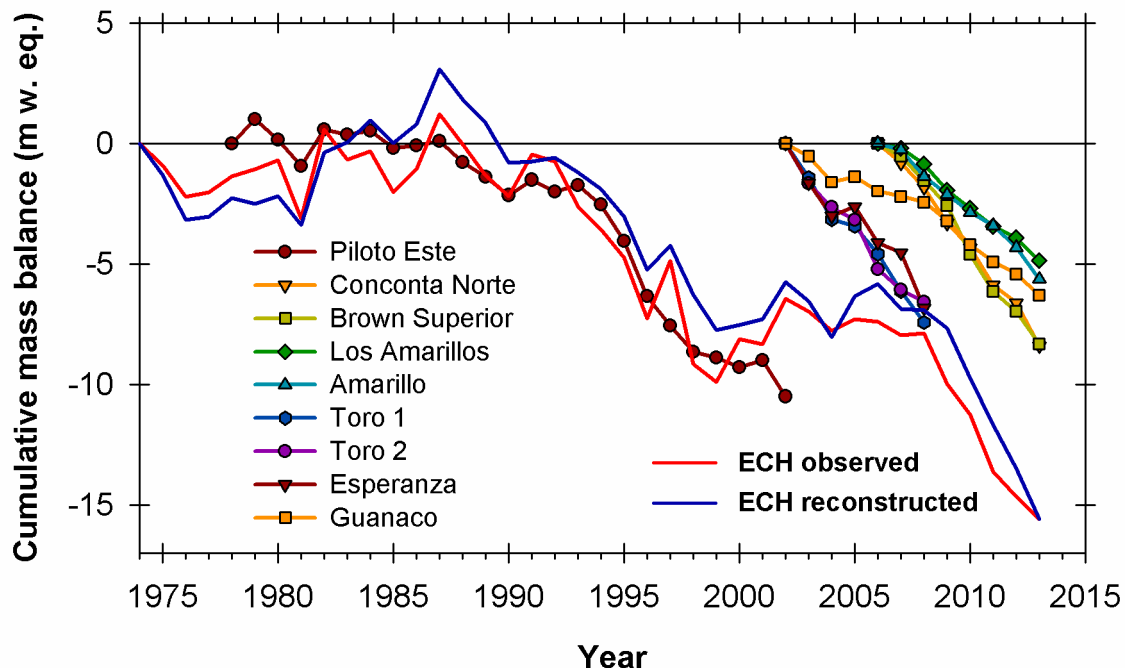
716  
717 **Figure 3.** (A) Winter and summer values observed at ECH between 1975 and 2012. (B) Annual  
718 mass balance series observed at ECH and modeled using El Yeso climate data (red and black  
719 lines, respectively). The estimated uncertainties of the modeled values ( $\pm 2 \text{ rmse}$ ) are shown with  
720 gray shading. (C) Annual mass balances observed at ECH (red line) compared to mass balances  
721 modeled using full variability in temperature but climatological monthly precipitation (dark red  
722 dashed line), and full variability in precipitation but climatological monthly temperatures (dark  
723 blue dashed line). Note the greater similarities between the observed series and the precipitation-  
724 based mass balance estimates.  
725



726

727 **Figure 4.** (A) Comparison between the annual mass balance record observed at ECH (red line)  
 728 and the reconstructed series derived from regionally-averaged streamflow data (blue line). The  
 729 estimated uncertainty of the reconstructed series ( $\pm 2 \varepsilon_{reco}$ ) is indicated by gray shading. (B)  
 730 Cumulative record of the observed and reconstructed ECH mass balance series (dark red and dark  
 731 blue lines, respectively). The initial value of the observed ECH cumulative record was modified  
 732 to match the corresponding value in the reconstructed series. The aggregated errors in this series  
 733 (see section 2.3) are also shown by gray shading (C) Glacier advances identified in the central  
 734 Andes of Chile and Argentina during the past 100 years (see text for details). Events are grouped  
 735 into 10-year intervals.

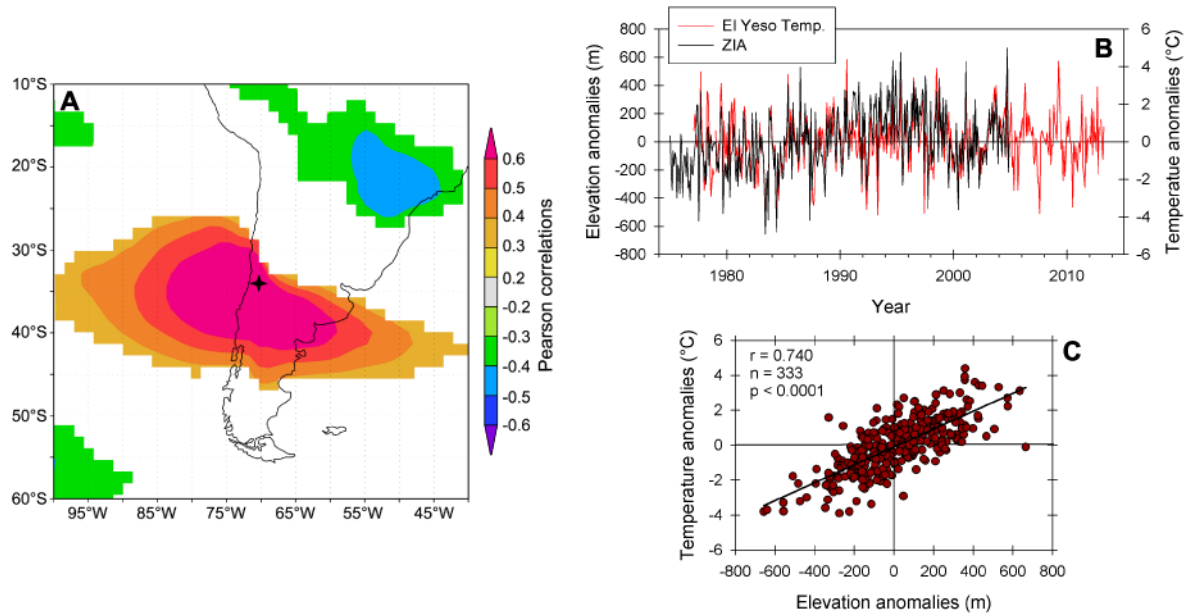
736



737

738 **Figure 5.** Comparison between the cumulative patterns in the observed and reconstructed records  
 739 from ECH and other glaciers with available direct mass balance data in the Dry Andes of Chile  
 740 and Argentina (Fig. 1 and Table 1).

741



742  
743 **Figure 6.** A) Map showing the correlations ( $p < 0.1$ ) between mean warm season (October-March)  
744 temperatures at the El Yeso station and gridded warm season ERA Interim mean temperatures for  
745 the 700 mb geopotential height level over the 1979-2012 period. The black star marks the  
746 location of the El Yeso station. B) Diagram showing variations of mean monthly temperatures at  
747 El Yeso (1977-2013) and the mean monthly elevation of the 0°C isotherm (ZIA) derived from  
748 radiosonde data from the Quintero coastal station (1975-2004). To facilitate the comparison, both  
749 series are expressed as anomalies from their mean seasonal cycles. C) Scatterplot of the El Yeso  
750 temperature and ZIA anomalies depicted in B. Note the positive, highly significant correlation  
751 between these two variables. ZIA data were provided by J. Carrasco from Dirección  
752 Meteorológica de Chile.  
753